

## Magnetic perturbation experiments on MAST using internal coils

A. Kirk, E. Nardon<sup>2</sup>, P. Tamain<sup>2</sup>, P. Denner, Yueqiang Liu, H. Meyer, S. Mordijck<sup>3</sup>, D. Temple and the MAST team

EURATOM/CCFE Fusion Association, Culham Science Centre, Abingdon, Oxon OX14 3DB, UK

<sup>2</sup>Association Euratom/CEA, CEA Cadarache, F-13108, St. Paul-lez-Durance, France

<sup>3</sup>University of California-San Diego, 9500 Gilman Dr, La Jolla, California 92093, USA

e-mail contact of main author: [andrew.kirk@ccfe.ac.uk](mailto:andrew.kirk@ccfe.ac.uk)

**Abstract.** Experiments have been performed on MAST using internal ( $n=3$ ) resonant magnetic perturbation coils. The application of the RMPs to L-mode discharges has shown a clear density pump out when the field line pitch angle at the low field side of the plasma is well aligned with the applied field. The size of the pump out seems to be correlated with the amplitude of the resonant component of the applied field. The toroidal rotation of the plasma does not affect the size of the density pump out. In type I ELM-ing H-mode discharges at a particular value of  $q_{95}$  the ELM frequency can be increased by a factor of 5 by the application of the RMPs. This effect on the ELMs is not correlated with the width of the region for which the (vacuum field) Chirikov parameter is greater than 1 but may be correlated with the size of the resonant component of the applied field in the pedestal region.

### 1. Introduction

In order to avoid damage to in-vessel components in future devices, such as ITER, a mechanism to reduce the size of type I ELMs is required.[1]. One such amelioration mechanism relies on perturbing the magnetic field in the edge plasma region, enhancing the transport of particles or energy and keeping the edge pressure gradient below the critical value that would trigger an ELM, while still maintaining an edge transport barrier. This technique of Resonant Magnetic Perturbations (RMPs) has been employed on DIII-D [2], where complete ELM suppression has been possible when pitch aligned fields are applied. On JET, where the magnetic perturbation applied has a broader spectrum, only ELM mitigation has been obtained [3]. A set of in-vessel ELM control coils consisting of two rows of six coils each, one above and one below the midplane, similar to the DIII-D I-coils, have been installed in MAST [4]. This paper presents results from the application of RMPs from an  $n=3$  configuration of these coils on MAST L and H-mode Connected Double Null (CDN) and Single Null Divertor (SND) discharges.

### 2. Effect of $n=3$ RMPs on L-mode plasmas

Initial experiments on Ohmic CDN L-mode plasmas, with a plasma current  $I_p=400\text{kA}$  and  $q_{95}=6.0$ , showed a clear density pump out due to the application of the RMPs (with a drop in  $n_e$  of up to 35%), together with an increase in the turbulent fluctuation level [4]. For this type of discharge the effect was only observed when the coils were in an even configuration (where the currents in the upper and lower coil at the same toroidal location have the same sign), and not in an odd configuration (the currents in the upper and lower coil have opposite sign). Calculations of the magnetic perturbation to the plasma due to the coils have been performed using the ERGOS code (vacuum magnetic modelling) [5]. The Chirikov parameter ( $\sigma_{ch}$ ), which is a measure of the island overlap, is used to define the stochastic layer as the region for which  $\sigma_{ch}$  is greater than 1 [5]. These calculations show that for this discharge

type, the even configuration is much more resonant than the odd one (with radial resonant perturbations larger by a factor  $>3$ ). The Chirikov parameter is a rather coarse measure of how the RMPs are interacting with the plasma and modifying the transport. For example, the size of the vacuum magnetic perturbation strength in these shots is similar to that in DIII-D discharges, however, the pump out observed is much smaller suggesting that different transport processes are important [6]. Similar to what has been observed on other devices, in these L-mode discharges the density pump out is accompanied by a splitting of the particle and heat flux to the strike point. A comparison of this splitting with modelling suggests that RMP penetration takes place [7].

The initial results presented in reference [4] have been extended to include measurements of the density pump out at higher initial density and as a function of toroidal field and of plasma rotation. Figure 1 shows the change in line averaged density ( $\bar{n}_e$ ) as a function of initial density due to the application of the RMPs in the even parity configuration with a coil current of 1.4 kA (5.6 kAt). The amplitude of the density pump out ( $\Delta\bar{n}_e$ ) decreases from a maximum of 35 % at low density to an approximately constant value at higher densities.

In order to investigate the effect of toroidal rotation on the density pump out, shots have been repeated with and without RMP with the addition of neutral beam heating to apply a torque to the plasma. The injection of 2 MW of beam power not only heats the plasma but increases the toroidal rotation from  $7 \text{ km s}^{-1}$  to  $25 \text{ km s}^{-1}$  near to the edge of the plasma ( $\Psi_N=0.95$ ). The pump out observed in these shots, shown as the triangles in Figure 1, is similar to that observed in shots at the same density without neutral beam injection. This suggests that there is little evidence that toroidal rotation, on its own, affects the screening of the RMPs by the plasma.

In addition, the line average density has been kept constant at  $\sim 3 \times 10^{19} \text{ m}^{-3}$  and an Ohmic shot repeated at different values of the toroidal field on axis:  $B_T=0.585$  (normal value), 0.54, 0.5 and 0.45T corresponding to values of  $q_{95}$  of 6.4, 6.0, 5.6 and 5.2. The density pump out measured is shown as the diamonds in Figure 1. Two points have an enhanced pump out i.e. have a  $\Delta\bar{n}_e \sim 0.25 \times 10^{19} \text{ m}^{-3}$  compared to the others which have  $\Delta\bar{n}_e \sim 0.12 \times 10^{19} \text{ m}^{-3}$ . These correspond to a repeated pair of RMP on/off shots, performed to ensure repeatability, at  $B_T=0.5 \text{ T}$  ( $q_{95}=5.6$ ). Thus it would seem that there is an optimum value of toroidal field ( $q_{95}$ ) that produces the largest pump out. ERGOS calculations show that the largest pump out is not correlated with the width of the stochastic region since this is largest in the highest  $B_T$  case.

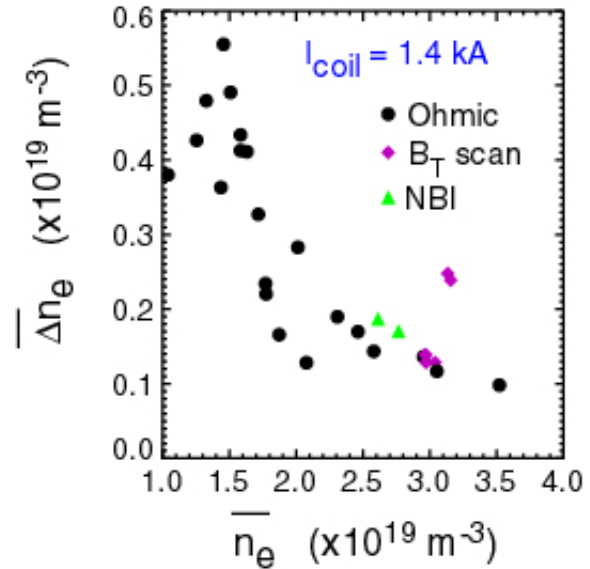


Figure 1 Dependence of the amplitude of the density pump out ( $\Delta\bar{n}_e$ ) as a function of line average density at a fixed coil current of 1.4 kA (5.6 kAt). The solid circles represent Ohmic discharges with an on axis toroidal field  $B_T=0.585\text{T}$ , the triangles NBI heated discharges with  $B_T=0.585\text{T}$  and the diamonds Ohmic discharges with a scan of  $B_T$  described in the text.

However, as the  $B_T$  is reduced the plasma becomes more pitch aligned with the applied perturbation, which leads to an increase in the size of the resonant component of the applied field in the pedestal region.

The effect on the edge plasma turbulence has been studied using a mid-plane reciprocating probe. The application of the RMPs produces a strong change in the ion saturation current fluctuations just inside the separatrix, with a broadening of the power spectrum and an asymmetrization of the probability distribution functions towards non-Gaussian shapes [8]. No major effect is found in the Scrape-Off Layer (SOL). The radial electric field profile flattens when the RMPs are applied, leading to an increase inside the separatrix and a decrease in the SOL. This change is consistent with what is expected from theories based on the establishment of a stochastic layer [9][10]. Given that the pump out and these phenomena appear to have the same existence threshold it seems likely that there is a modification of the turbulent transport level. This is in agreement with results from B2SOLPS modelling which show that the transport coefficients have to be increased in order to match the observed pump out and changes in electric field [9].

The effect of the coils has also been studied in other plasma configurations, for example, it is also possible to produce a density pump out using the coils in an odd parity configuration in a shot with  $I_p = 900$  kA where again the pitch angle at the low field side is well aligned with the coils. In shots with  $I_p = 750$  kA, the pitch angle alignment is marginally

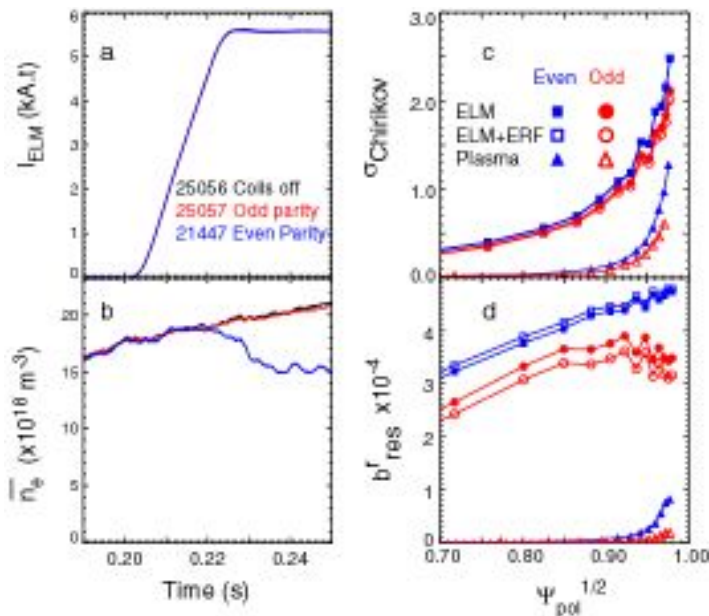


Figure 2 Time traces of a) coil current ( $I_{ELM}$ ) and b) line average density ( $\bar{n}_e$ ) for an L-mode shot with 750 kA plasma current using coils in odd and even parity mode. Calculated profiles of c) the Chirikov parameter and d) the normalised resonant component of the applied field ( $b_r^{res}$ ) produced with 5.6 kAt in the ELM coils. The calculations have been done for the ELM coils only and including the intrinsic plus error field correction fields in the vacuum approximation and taking into account the plasma response.

better for even than odd parity but neither is ideal. The Chirikov parameter profile for both configurations is similar (see figure 2c), with both predicted to have a large region for which the  $\sigma_{Chirikov} > 1$ . However, a density pump out is only observed in the even parity configuration (see figure 2a and b).

The only noticeable difference from the vacuum modelling is that the normalised resonant component of the applied field ( $b_r^{res}$ ) is larger in the case of even parity (see figure 2d). In order to see how the other non-axisymmetric fields affect these calculations, the fields from the intrinsic error fields and the error field correction coils have been added to those produced by the ELM coils and included into the ERGOS modelling. The Chirikov parameter profile is little altered by the addition of these fields (figure 2c) but the small difference in the initial  $b_r^{res}$  profile is increased (see figure 2d). However, this change is

insignificant compared to the change that occurs when the plasma response is considered.

Calculations have been performed using the MARS-F code, which is a single fluid resistive MHD code [11] that combines the plasma response with the vacuum perturbations, including screening effects due to toroidal rotation. These calculations show an amplification of the non-resonant ( $m < 0$ ) components (i.e. the modes that have opposite helicity to the field lines) but a significant reduction in the resonant components due to screening effects. The calculations use the experimental profiles of density, temperature and toroidal rotation as input and realistic values of resistivity, characterised by the Lundquist number ( $S$ ) which varies from  $10^8$  in the core to  $10^6$  at the edge. The resonant component of the field reduces by more than an order of magnitude (figure 2d) with the reduction being largest in the case of odd parity. The Chirikov parameter profile is also reduced and the Chirikov parameter only just exceeds 1 at the edge of the profile and only in the case of even parity. In the MARS-F modelling the RMP field also causes a 3D distortion of the plasma surface and in all the shots considered density pump-out only occurs when the surface plasma displacement peaks near the X-point [11].

### 3. Effect of $n=3$ RMPs on L-H transition

Since it will be necessary to suppress the first large type I ELM in ITER, the RMPs may need to be applied before the L-H transition, which may affect the power required to access H-mode. On MAST the application of  $n=3$  RMPs before the L-H transition can either suppress the L-H transition entirely or significantly delay it. Figure 3 shows an example from shot 24560 which with 1.8 MW of beam power and without the application of RMPs goes into a

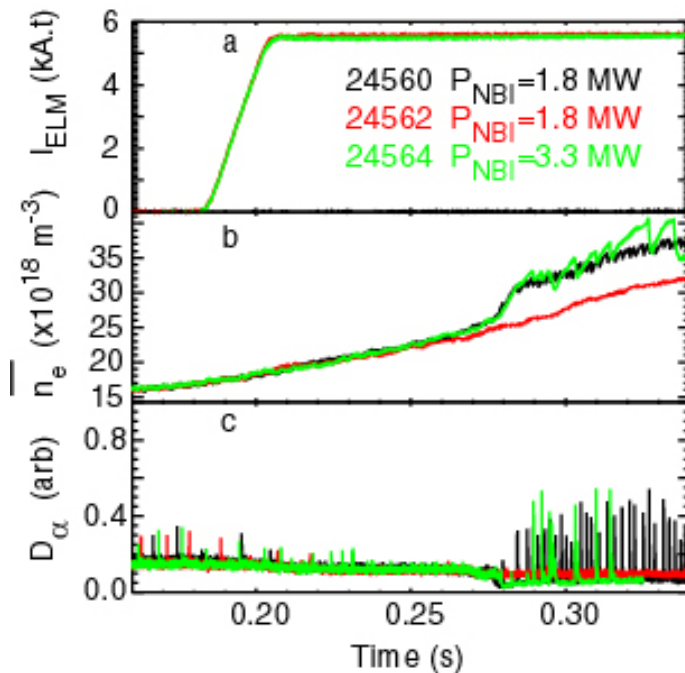


Figure 3 Time traces of a) coil current ( $I_{ELM}$ ) b) line average density ( $\bar{n}_e$ ), and c)  $D_\alpha$  for shot 24560 without RMPs and with 1.8 MW Neutral Beam heating and for shots 24562 and 24564 with RMPs and with 1.8 and 3.3 MW of neutral beam heating respectively.

type III ELMy H-mode at 0.27 s. If all the plasma parameters are kept constant and an  $n=3$  RMP is applied with 5.6 kAt before the time of the L-H transition, as in shot 24562, the H-mode transition is completely suppressed. To restore the H-mode the beam power has to be increased by  $\sim 33\%$  i.e. to 2.4 MW and in this case (not shown) the H-mode transition is delayed by  $\sim 80$  ms. In order to produce an L-H transition at the same time as in the shot without the coils the beam power has to be raised to 3.3 MW (i.e. an increase of  $\sim 80\%$ ) as in shot 24564 shown in Figure 3.

In all discharge types investigated, it is found that the application of  $n=3$  RMPs, with an amplitude sufficient to stochastise a layer with a width  $\Delta\psi_{pol} > 0.17$  (according to vacuum field modelling), before the L-H transition requires at least a 30 – 40 % increase

component ( $\vec{v} \times \vec{B}$ ) of the radial electric field ( $E_r^{v \times B}$ ), which has been measured using active Doppler spectroscopy of  $\text{He}^+$  at the low field side midplane with a radial spatial resolution of 1.5 mm and a temporal resolution of 5ms. For example, in shot 24560 (without RMPs) the  $E_r^{v \times B}$  remains approximately constant up until the time of the L-H transition. In shot 24562 (with RMPs), the  $E_r^{v \times B}$  is identical initially but as the RMPs are applied the  $E_r^{v \times B}$  increases (becomes more positive) by  $\sim 2 \text{ kVm}^{-1}$  and remains high at the time that shot 24560 transitions into H-mode. If the RMP applied was off resonance (i.e. in this case an odd parity configuration was used) or the coil current was below a threshold value (4 kAt for this discharge) then there was no change in the radial electric field or in the H-mode access.

#### 4. Effect of n=3 RMPs on connected double null H-mode plasmas

In H-mode, for CDN plasmas just above the L-H transition threshold, the application of the coils seems equivalent to a small decrease in input power. For example, the application of the RMPs can trigger more frequent ELMs in a type III ELMing discharge and can trigger type III ELMs in an ELM free discharge [4]. Initial experiments showed that the application of the RMPs to discharges with type I ELMs produced little effect on the ELM behaviour or pedestal characteristics. This was despite the fact that vacuum modelling using the ERGOS code showed that the stochastised layer (defined as the region for which the Chirikov parameter is greater than 1) had a radial extent wider than that correlated with ELM suppression in DIII-D [12]. However, there are many differences between the MAST and DIII-D discharges, including shape, aspect ratio and collisionality so if these parameters are important ELM suppression may not be achieved on MAST.

More recent experiments have shown that it is possible to increase the ELM frequency and decrease the ELM energy loss

by carefully adjusting the  $q_{95}$  of the plasma. Figure 4 shows a series of shots where the  $q_{95}$  is lowered from 5.4 to 4.5, while an n=3 RMP was applied in odd parity (which is predicted to be more on resonance at lower  $q_{95}$ ) with a peak value of 5.6 kAt in the coils from a time of 0.24 s. For the shots with  $q_{95} = 5.4$  and 5.1 there is very little effect, however, for the shot with  $q_{95} = 4.9$  a drop in density is observed around 0.3 s and the ELM frequency increases. For lower  $q_{95}$  a back transition to L-mode is observed before any impact on the ELMs can be established. The back transition occurs at  $t=0.315 \text{ s}$  for  $q_{95} = 4.7$  and  $t=0.28 \text{ s}$  for  $q_{95}=4.5$ . The shots have also been repeated with no RMPs

applied and in this case there was very little change in the ELM behaviour or H-mode duration with  $q_{95}$ . The shot with  $q_{95}=4.9$  has been repeated several times and the properties of the ELMs before and after the change in frequency established. Up until the sharp density pump out at 0.3 s the shots with and without RMPs have similar density, temperature and

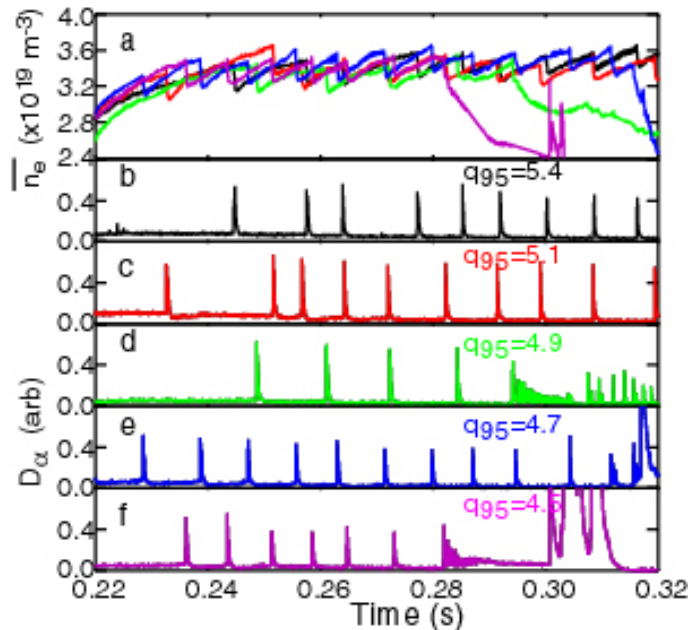


Figure 4 Time traces of a) line average density ( $\bar{n}_e$ ), and b-f)  $D_\alpha$  for shots with  $q_{95}$  in the range 5.4 to 4.5.

toroidal velocity profiles. Just after the density drop there is again little change in the velocity or temperature (ion or electron) profiles while the pedestal density decreases by  $\sim 30\%$ . The pedestal characteristics move from those associated with type I ELMs on MAST to those previously found to be associated with type IV ELMs [13]. A similar effect has also been observed during Double Null discharges in DIII-D [14]. The net loss in pedestal pressure means that the stored energy reduces from 120 kJ to 106 kJ, while the ELM frequency ( $f_{\text{ELM}}$ ) increases from  $\sim 100$  to  $\sim 500$  Hz and the energy loss per ELM ( $\Delta W_{\text{ELM}}$ ) decreases from a mean value of  $\sim 5$  kJ to  $\sim 1$  kJ i.e. consistent with  $\Delta W_{\text{ELM}} \cdot f_{\text{ELM}} \sim \text{constant}$ .

ERGOS modelling shows that as the  $q_{95}$  is lowered the magnetic perturbations become more well aligned with the plasma  $q$  profile and the normalised resonant component of the applied field ( $b_r^{\text{res}}$ ) in the pedestal region increases from  $5 \times 10^{-4}$  for  $q_{95}=5.4$  to  $7 \times 10^{-4}$  for  $q_{95}=4.9$ . However, the width of the stochastic layer does not change (i.e. the Chirikov profile remains about the same) due to the fact that although the resonant field is increasing, the island overlap decreases due to the reduction in  $q_{95}$  and of the edge shear. This may indicate that the Chirikov parameter is not the main parameter in determining whether or not ELM mitigation is established but it may be that either the resonant component of the field or the alignment between the plasma magnetic field pitch angle and the applied perturbation is more important. Similar, strong dependences of the observed effect on  $q_{95}$  have been observed on DIII-D [15] and JET [16].

### 5. Effect of $n=3$ RMPs on single null divertor H-mode plasmas

To investigate if magnetic geometry can influence the effect of RMPs on ELM behaviour, SND discharges have been investigated. Due to the up-down symmetry in the divertor coils on MAST, SND discharges are usually produced by shifting the plasma downwards (see

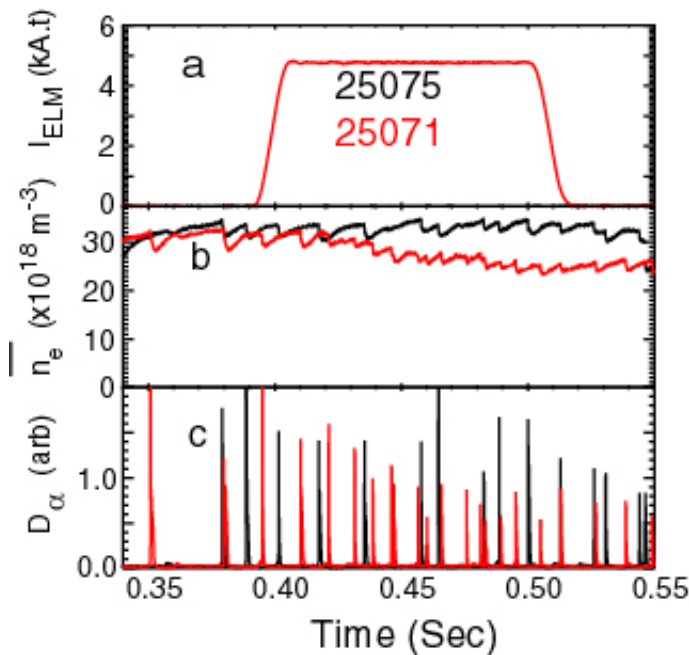


Figure 5 Time traces of a) the coil current ( $I_{\text{ELM}}$ ) b) line average density ( $\bar{n}_e$ ), and c)  $D_\alpha$  for the lower SND shots.

Figure 6a). In this lower SND magnetic configuration the plasma is far from the upper row of coils and hence the perturbation is predominantly from the lower row of coils, which produces a much broader spectrum of magnetic perturbation. If the RMPs are applied with full current in both the upper and lower row of coils then a brief increase in the ELM frequency and decrease of the ELM size is observed, together with a decrease in the plasma density. Unfortunately this is then followed by a back transition to L-mode due to the fact that the RMPs cause a large braking to the toroidal plasma rotation, which is observed to extend all the way into the core of the plasma. ERGOS calculations show that the maximum of the applied RMP can be shifted radially outwards by changing the ratio of the upper to lower currents (decreasing the lower coil current) and shifting the plasma vertically upwards by 2 cm. This does reduce the braking substantially and has enabled the period with smaller ELMs to be maintained for up to 100 ms (see Figure 5). In this discharge

the ELM frequency increases from 80 to 150 Hz, while the ELM energy loss decreases from 10 kJ to 6kJ. The pedestal density decreases from 3 to  $2.5 \times 10^{19} \text{m}^{-3}$  and the pedestal temperature remains unaltered at 300 eV which results in a 15 % decrease in stored energy.

Much of the work on DIII-D on ELM mitigation has been performed in an ITER like shape. It has been found possible to reproduce this shape on MAST by modifying the divertor coil configuration, breaking the up-down symmetry and putting the solenoid current in series with one of the divertor coils. The shape that is produced is shown in Figure 6a compared to the DIII-D ITER like shape, which has been shifted radially by 0.8m. The shape match is quite good except near the X-point. This has resulted in an on-axis SND plasma that is now close to both rows of coils

The drawback to this configuration is that the divertor currents have to be constrained in order to reduce axial forces on the solenoid, which has restricted the plasma current to 600 kA. The Chirikov profiles are shown in Figure 6b and as can be seen the predicted stochastic layer is large for both parities and is well aligned with an even parity configuration of the coils. A density pump out of 20 % is observed in L-mode in even parity at moderate current in the coils (4 kAt). If the current is increased above this, even though an  $n=3$  RMP is applied, an  $n=1$  locked mode is triggered.

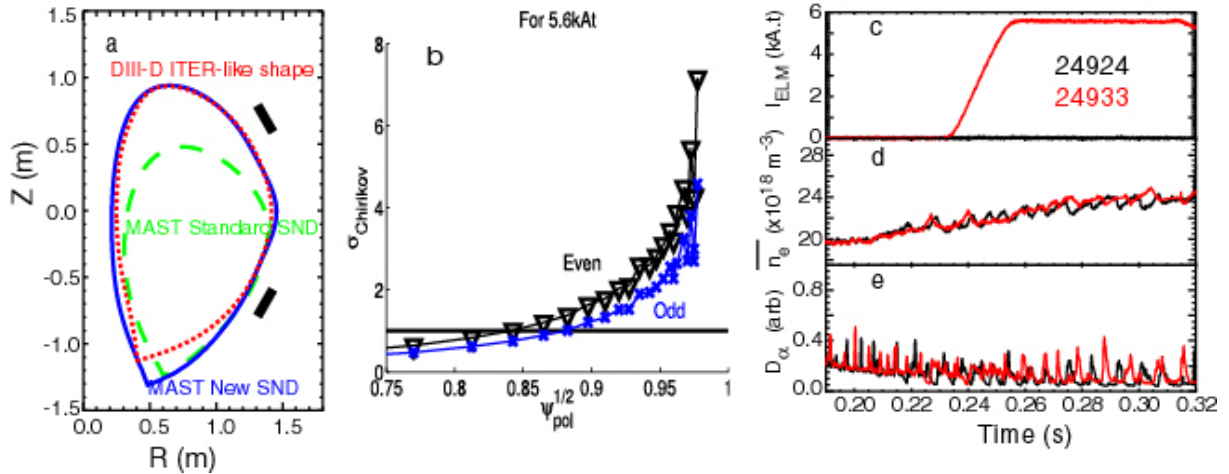


Figure 6 a) Poloidal profiles of the SND discharge scenarios with the location of the internal coils indicated. b) Calculated profiles of the Chirikov parameter produced with 5.6 kAt in the ELM coils in even (triangles) and odd (crosses) parity configurations. Time traces of c) the coil current ( $I_{ELM}$ ) d) line average density ( $\bar{n}_e$ ), and e)  $D_\alpha$  for shots in the DIII-D ITER like shape.

As has been observed in other configurations, the application of the RMPs before the L-H transition suppresses H-mode and requires an increase of 30 – 40 % in beam power to restore the transition. Similar to what was observed in the original CDN experiments the application of the coils during type I ELM-ing H-mode has very little effect on the ELMs (see Figure 6c), despite the large predicted stochastic layer width. Unfortunately due to the restrictions on this shot it has not been possible to perform a  $q_{95}$  scan so it is not clear whether a particular  $q_{95}$  value would have an effect on the ELMs. What is clear is that in this shape it is no easier to have an effect on the ELMs than in the other shapes investigated.

## 6. Summary and conclusions

Experiments have been performed on MAST using internal ( $n=3$ ) resonant magnetic perturbation coils. Vacuum modelling with ERGOS showed that these coils could produce a region  $\psi_{pol}^{1/2} > 0.91$  for which the Chirikov parameter is greater than 1. The application of the

RMPs to L-mode discharges has shown a clear density pump out when the pitch angle at the low field side of the plasmas is well aligned with the coils. The size of the pump out seems to be correlated with the maximum size of the resonant component of the applied field. The size of the pump out is not affected by an increase in toroidal rotation of the plasma suggesting that any screening effects are already saturated at the lower value.

In type I ELM-ing H-mode plasmas an effect on the ELM frequency and size has been observed at particular  $q_{95}$  values. In the best example seen to date the ELM frequency is increased by a factor of 5. The scan shows that the effect is not correlated with the width of the region for which the Chirikov parameter is greater than 1 but again seems to be related to the size of the resonant field component in the pedestal region. One possible explanation is that the Chirikov parameter goes as the square root of the RMP amplitude, however, what is important is whether or not the RMPs penetrate the plasma. The penetrated field may go as the square of the RMP amplitude because the braking torque exerted by the RMP on the resonant surfaces goes as the induced helical current times the local RMP, which both go as the applied vacuum RMP. Hence this may explain why optimising the resonant component not only increases the pump out in L-mode it also leads to ELM mitigation in H-mode.

### Acknowledgements

This work was funded by the RCUK Energy Programme under grant EP/G003955 and the European Communities under the contract of Association between EURATOM and CCFE. The views and opinions expressed herein do not necessarily reflect those of the European Commission.

### References

- [1] Loarte A *et al.*, 2003 *Plasma Phys. Control. Fusion* **45** 1594
- [2] Evans T. *et al.*, 2004 *Phys. Rev. Lett.* **92** 235003
- [3] Liang Y. *et al.*, 2007 *Phys. Rev. Lett.* **98** 265004
- [4] Kirk A. *et al.*, 2010 *Nucl. Fusion* **50** 034008
- [5] Nardon E. *et al.*, 2007 *J. Nucl. Mater.* **363-365** 1071
- [6] Mordijck S. *et al.*, "Comparison of resonant magnetic perturbation induced particle transport changes on DIII-D and MAST" To be published in *J. Nucl. Mater.*
- [7] Nardon E. *et al.*, 2009 *Plasma Phys. Control. Fusion* **51** 124010
- [8] Tamain P. *et al.*, 2010 *Plasma Phys. Control. Fusion* **52** 075017
- [9] Rozhansky V. *et al.*, *Nucl. Fusion* **50** (2010) 034005
- [10] Tokar M.Z. *et al.* *Phys. Plasmas* **15** (2008) 072515
- [11] Liu Yueqiang *et al.*, "Modelling of Plasma Response to RMP Fields in MAST and ITER", Paper THS/P5-10, Proc. 23rd IAEA Fusion Energy Conference 2010, Daejeon Korea
- [12] Fenstermacher M.E. *et al.* 2008 *Phys. of Plasma* **15** 056122
- [13] Kirk A. *et al.*, 2009 *Plasma Phys. Control. Fusion* **51** 065016
- [14] Hudson B. *et al.*, 2010 *Nucl. Fusion* **50** 064005
- [15] Schmitz O. *et al.*, 2010 *Phys. Rev. Lett.* **103** 165005
- [16] Liang Y. *et al.*, 2010 *Phys. Rev. Lett.* **105** 065001